In vivo study of polyurethane and tannin-modified hydroxyapatite composites for calvarial regeneration

Xinggui Tian[1,2*], Xiaowei Yuan[1,3*], Daxiong Feng[2*], Min Wu[1], Yuping Yuan[4], Chuying Ma[5], Denghui Xie[1], Jinshan Guo[1], Chao Liu[5] and Zhihui Lu[1] (iD)

Abstract

Biomaterial mediated bone regeneration is an attractive strategy for bone defect treatment. Organic/inorganic composites have been well established as effective bone graft. Here, the bone regenerative effect of the composites made from tannic acid (TA) modified hydroxyapatite (HA) (THA) or TA & silver nanoparticles (Ag NPs) modified HA (Ag-THA) and polyurethane (PU) was evaluated on critical-sized calvarial defects in rats. The in vivo study indicates that PU/THA and PU/Ag-THA scaffolds exhibited acceptable biocompatibility and induced significantly enhanced bone mineral densities comparing with the blank control (CON) group as well as PU/HA group. The inclusion of TA on HA brought the composites with enhanced osteogenesis and angiogenesis, evidenced by osteocalcin (OCN) and vascular endothelial growth factor (VEGF) immunohistochemical staining. Tartrate resistant acid phosphatase (TRAP) staining showed high osteoclast activity along with osteogenesis, especially in PU/THA and PU/Ag-THA groups. However, further introduction of Ag NPs on HA depressed the angiogenesis of the composites, leading to even lower VEGF expression than that of CON group. This study once more proved that THA can serve as a better bone composite component that pure HA and can promote osteogenesis and angiogenesis. While, the introduction of antimicrobial Ag NPs on HA need to be controlled in some extent not to affect the angiogenesis of the composites.

[1]Department of Histology and Embryology, School of Basic Medical Sciences, Guangdong Provincial Key Laboratory of Bone and Joint Degeneration Diseases, The Third Affiliated Hospital of Southern Medical University, Southern Medical University, Guangzhou, China

[2]Department of Orthopaedics, The Affiliated Hospital of Southwest Medical University, Luzhou, Sichuan, P. R. China

[3]Department of Orthopedics, Shengjing Hospital of China Medical University, Shenyang, China

[4]Department of Material Science and Engineering, Southern University of Science and Technology, Shenzhen, China

[5]Aleo BME, Inc., State College, PA, USA

*These authors contributed equally to this work.

Corresponding authors:

Denghui Xie, Department of Histology and Embryology, School of Basic Medical Sciences; Guangdong Provincial Key Laboratory of Bone and Joint Degeneration Diseases, The Third Affiliated Hospital of Southern Medical University, Southern Medical University, Guangzhou 510515, China
Email: smuspine@163.com

Chao Liu, Aleo BME, Inc., 200 Innovation Blvd, Suite 210A, State College, PA 16803, USA.
Email: ch.liu@aleobme.com

Zhihui Lu, Department of Histology and Embryology, School of Basic Medical Sciences, Guangdong Provincial Key Laboratory of Bone and Joint Degeneration Diseases, The Third Affiliated Hospital of Southern Medical University, Southern Medical University, 1023 Shatai Nanlu, Guangzhou 510515, China.
Email: sanlumo12@smu.edu.cn

Introduction

The cause of human bone defect is mainly due to aging, tumor, trauma and other factors.[1–3] Most bone defects cannot recover by themselves, bone transplantation is always needed.[2–7] Traditional bone defect treatment or bone replacement includes autografts and allografts and the substitute tissues could rapidly osseointegrate with surrounding tissues after implantation.[7] However, conventional bone therapy has encountered limitations such as the threat of bone disease spread, immune response, donor deficiency, and donor site morbidity.[2–8] Alternatively, artificial bone grafts are promising to repair bone defects. Elaborately designed artificial bone grafts should be biocompatible and biodegradable as well as osteoconductive, osteoinductive and angiogenesis promoting, providing temporary and gradually regressive substitutes in the bone defect sites, and actively promote bone regeneration in the degradation process.[2,5,9–18] However, the fabrication of ideal bone grafts are still challenging.

In the past few decades, the innovation in the field of artificial bone grafts has stimulated research on bone tissue engineering. The ideal tissue engineered biomimetic materials for bone regeneration should possess excellent osteoconductivity, the ability to promote osteoblast differentiation and osteogenesis.[9] In order to mimic the integrated inorganic/organic chemical components of natural bone, biomemitic artificial bone materials are usually composed of hydroxyapatite (HA, $Ca_{10}(PO_4)_6(OH)_2$) and the organic polymeric scaffold.[19] HA is an important inorganic component of bone and due to its biocompatibility as well as cell adhesion properties, hydroxyapatite is used as a ceramic biomaterial for artificial bone materials. Polyurethane (PU) has been selected as biomaterial to repair bone and cartilage since late 1990s, as cement, injectable space fillers, scaffold, drug delivery systems and shape memory materials.[20] It possesses the property of easy chemical and physical modification and has excellent mechanical as well as physicochemical flexibility that the characteristics of PU can be customized by changing chemical composition, raw material ratio, and synthesis or process parameters.[21] Properly designed PUs are non-toxic, biocompatible and they can promote biomineralization in the body that make it an excellent candidate for artificial bone scaffold material.[21,22]

In order to increase the compatibility between the inorganic HA and the organic polymer and maintain the artificial bone structure embedded in bone defect, HA surface "organic" modification, such as with lactic acid (LA) oligomers,[23,24] poly(amino acid)[25] or poly(N-isopropylacryla-mide) (PNIPAM),[26] is always necessary. Tannic acid (TA) is a plant-derived hydrolyzable polypehnol with favourable biological functions, such as antimicrobial, antiviral, anticancer, anti-inflammatory and antioxidant properties.[27] Previously, by employing tannin-inspired adhesion strategy, an universal and facile HA surface "organic" modification approach with tannic acid (TA) was developed in our Lab, to confer the modified HA with improved compatibility to organic polymer, enhanced biomineralization performance and considerable antimicrobial activity.[17] Silver nanoparticles (Ag NPs) can also be conveniently immobilized onto the surface of HA, to enhance the antimicrobial activity.

In this study, an alternating block PU (Alt-PU) with poly(ε-caprolatone) (PCL) and poly(ethylene glycol) (PEG) blocks alternately distributing in the polymer chain (PUCL-alt-PEG), which possesses better mechanical strengths and exhibited better wound healing efficiency exemplified in never regeneration than its random counterparts, was chosen as an representative PU.[28–31] Alt-PU was used to composite with TA modified HA (THA) and Ag NPs & TA modified HA (Ag-THA) to fabricate PU/THA, PU/Ag-THA porous composite microparticulates (MPs) for critical-sized calvarial defect regeneration on rats. The osteogenesis and angiogenesis of these composite MPs were evaluated by micro-computed tomography (μ-CT), H&E, Masson's trichrome and Safranin O/fast green staining, OCN and VEGF immunohistochemical staining. The effect of the composite MPs to osteoclast was also assessed by tartrate resistant acid phosphatase (TRAP) staining.

Experimental section

Materials

Hydroxyapatite (HA), tannic acid (TA), silver nitrate ($AgNO_3$) and other chemicals were all purchased from Sigma-Aldrich, and used without further purification. PUCL-*alt*-PEG was synthesized according to literatures previously reported, the molecular weight of PUCL-*alt*-PEG was ~40 KDa.[28–31] THA and Ag-THA were synthesized according to our previous work.[19]

Composite microparticulates (MPs) fabrication

The porous PU/HA, PU/THA and PU/Ag-THA scaffolds (porosity: 80%, pore size: 250–425 μm) in a cuboid shape (50 × 50 × 2 mm) were fabricated using salt leaching method.[2,17] Briefly, 8.0 g sodium chloride (NaCl) crystals (250–425 μm, as a porogen), 1.0 g Alt-PU (in 10 mL 1, 4-dioxane) and 1.0 g HA, THA or Ag-THA (50 wt% of the total weight of HA or modified HA and dry polymer) were mixed and stirred to evaporate the solvent at room temperature, until the mixture became an even viscous liquid. Then the mixture was fitted into a cuboid Teflon mold (50 × 50 × 2 mm). After drying in a chemical hood for more than 2 days, the scaffold was soaked in deionized water until the salt was all removed. Then the scaffold samples were freeze-dried, grounded and sieved to collect the microparticles (MPs) with sizes between 250 and 425 μm, which were sterilized by ethylene oxide for the following animal study (Scheme 1).
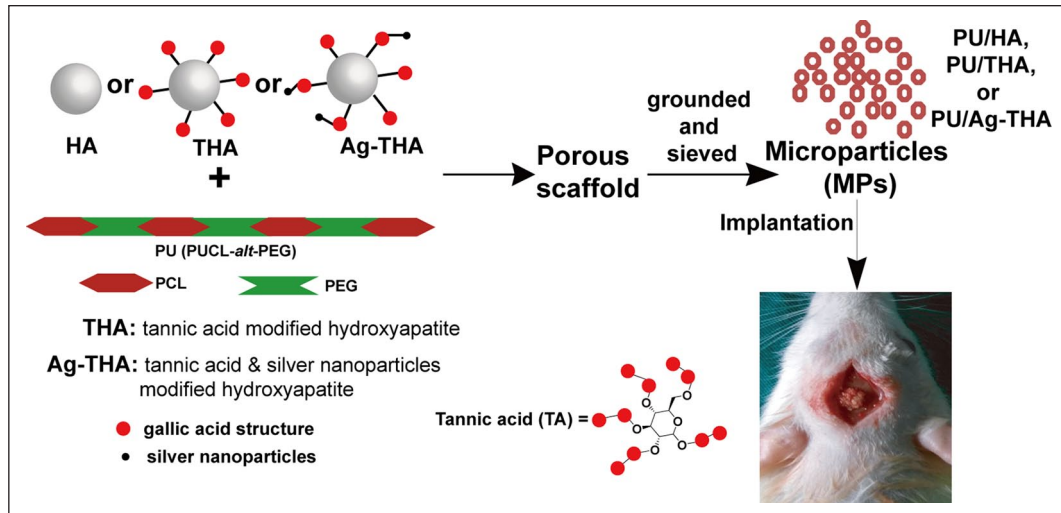
Scheme 1. Fabrication of PU/HA, PU/THA and PU/Ag-THA composite microparticles (MPs) and the application of them for calvarial regeneration on rats.

In vivo bone regeneration study

Adult male Sprague-Dawley (SD) rats (220–250 g, purchased from the Experimental Animal Center of Southern Medical University, Guangzhou, China) were used for the following animal experiments. All surgical procedures as well as perioperative handling were conducted in accordance with protocols approved by the Ethics Committee at the Southern Medical University.

Rat critical-size calvarial defect model and scaffold implantation

75 SD rats were randomly assigned to PU/HA, PU/THA, PU/Ag-THA, autograft bone (AB) and blank control (CON) groups, with 15 SD rats in each group. Anesthesia of SD rats was induced by the intraperitoneal injection of 100 mg/kg chloral hydrate. After full shaving and sterilization, a sagittal incision in the middle of the surgical area was made, and then soft tissue and periosteum were carefully separated to expose the calvarium. A 5 mm diameter defect was carefully created on calvarium with a trephine drill, which was constantly cooled with sterile saline. The calvarial disk was then carefully removed to avoid tearing of the dura. In the autograft bone transplantation group (AB), the harvested calvarial disk was put back to the defect area. In the CON group, the defect area was left empty, and served as a negative control (Figure 1(a)–(c)). In PU/HA, PU/THA, and PU/Ag-THA groups, the defects were filled with the prefabricated scaffold samples, and saline was used to make the scaffold closely fit the bone defect (Scheme 1). Then the periosteum, soft tissue and skin were sutured. After surgery, penicillin was injected once a day for 3 days to avoid infection.

Microcomputed tomography (μ-CT) analysis

At week 4, 8, and 12 post operation, SD rats were euthanatized, the calvarial specimens were harvested and fixed in 4% paraformaldehyde for further study. Micro-CT (Aloka Latheta LCT-200, Hitachi-Aloka Medical, Ltd., Japan) was used in an isolated bone mode to evaluate the bone regeneration in the defect area with the following settings: pixel size, 480 μm; slice thickness, 240 μm; slice pitch, 240 μm; speed, integ. 2; rotation angle, 360°; X-ray voltage, low; artifact removal, lean; sync. scan, no; metal artifact reduction, no. The three-dimensional (3D) and two-dimensional (2D) images of the regenerated calvarium sections were reconstructed using VGStudio MAX software (version 2.2.2). A cylinderic space representing the volume of interest (VOI) was designated to evaluate new bone formation by calculating bone mineral density (BMD) using Latheta software (Hitachi Aloka Medical Ltd., Japan).

Histological analysis

The fixed specimens were decalcified in 10% ethylenediamine tetraacetic acid (EDTA, pH 7.4) for 30 to 60 days at 37°C, followed by alcohol gradient dehydration, dimethyl benzene substitution and paraffin embedding. The embedded specimens were sliced into 4 μm-thick histological sections, hematoxylin and eosin (H&E), Masson's trichrome and Safranin O/fast green staining were conducted. Tartrate resistant acid phosphatase (TRAP) staining was conducted to assess osteoclast activity using Acid Phosphatase, Leukocyte (TRAP) Kit form Sigma-Aldrich. Methyl green was used to replace hematoxylin for cell nuclei staining, to give prominence to TRAP positive cells
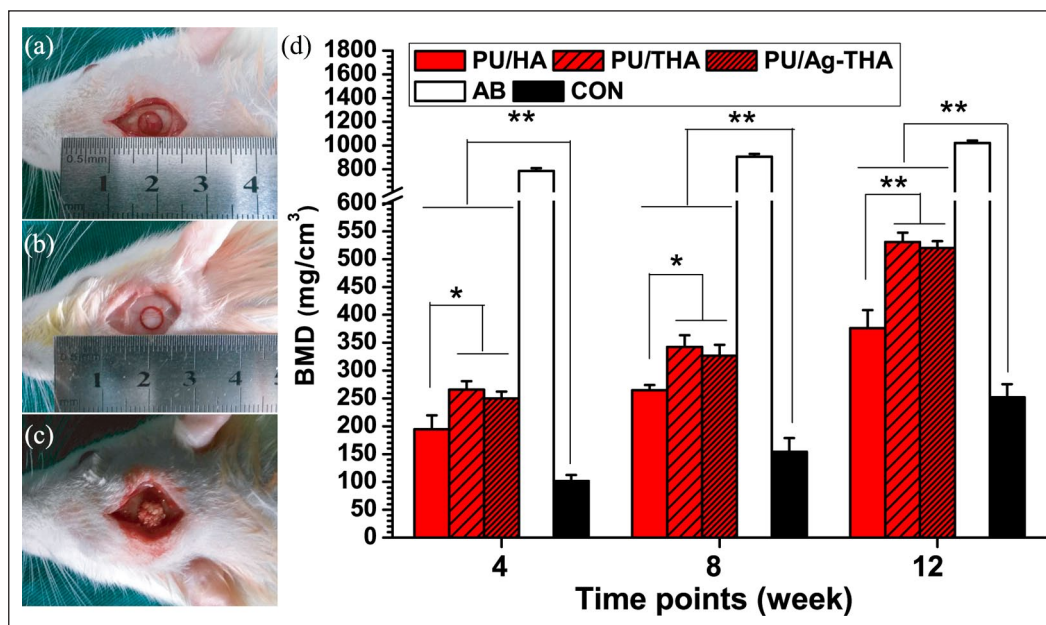
Figure 1. (a) Representative photographs showing the created cylindrical calvarial defect (5 mm in diameter) on rat. (b) The implantation of autograft bone (AB) in the defect. (c) The implantation of porous scaffold in the defect. (d) Bone mineral densities (BMDs) of different samples at week 4, 8, and 12 post surgery.

AB: autograft bone; CON: no implantation in the defect.

*p < 0.05, **p < 0.01.

labeled in purplish red. Osteocalcin (OCN) and vascular endothelial growth factor (VEGF) immunohistochemical staining were used to access the osteogenesis and angiogenisis in the defect area, respectively. The stained tissue sections were observed and photographed under bright field microscope (Axio Scope A1, Carl Zeiss Microscopy GmbH, Jena, Germany). The numbers of OCN positive cells per millimeter of bone perimeter and the mean optical densities of VEGF positive cells for different samples at different time points were calculated from the OCN and VEGF stained images respectively using ImageJ. Cells were counted from at least six different areas from more than three tissue sections, and the results are shown in Figure 5(c) and (d) respectively.

Statistical analysis

Data were analyzed using SPSS statistics 20 statistical software (SPSS, Inc., Chicago, IL, USA). All quantitative results are expressed as mean ± standard deviation. The statistical significance between two sets of data was determined by one-way analysis of variance (ANOVA). Data were taken to be significant if $p < 0.05$ (*) was obtained.

Results and discussion

Previously, tannin-inspired adhesion strategy was employed by us to bridge organic and inorganic phases together for biomimetic bone composite development.[17] Through facile one-step surface coating process, tannic acid (TA) is adhered to the surface of hydroxyapatite (HA), silver nanoparticles (Ag NPs) in situ reduced by TA can also be simultaneously immobilized on the surface of HA. Residual functional groups on TA was used to covalently link to citrate-based biodegradable polymer, to effectively bridge the organic and inorganic phases, conferring the obtained citrate-based tannin-bridged bone composites (CTBCs) with greatly improved compression strengths, as well as considerable antimicrobial activity.[17] However, citrate-based polymers themselves also possessed some antimicrobial property, the universal application of tannin modified HA in bone composite with non-antimicrobial polymers has never been thoroughly investigated in vivo. As Hollinger et al. pointed out that if the ratio of defect size to bone diameter is more than 1.5, nonunion will occur,[29] the critical-sized calvarial defect model is one of the most widely used models for testing the osteogenic potential of orthopedic materials. Herein, tannic acid (TA) modified HA (THA) or Ag NPs and TA modified HA (Ag-THA) were used to composite with a non-antimicrobial, biocompatible and relatively hydrophilic polyurethane (PU), alternating block polyurethane (Alt-PU) based on PCL and PEG (PUCL-alt-PEG),[26–28] to obtain PU/THA and PU/Ag-THA porous composites MPs, and used for critical-sized calvarial regeneration on rats (Figure 1(a)). The degradation of PUCL-alt-PEG is relatively slow according to previous literatures,[26–28] suitable to be used for bone regeneration. PU/HA MPs, autograft bone (AB,
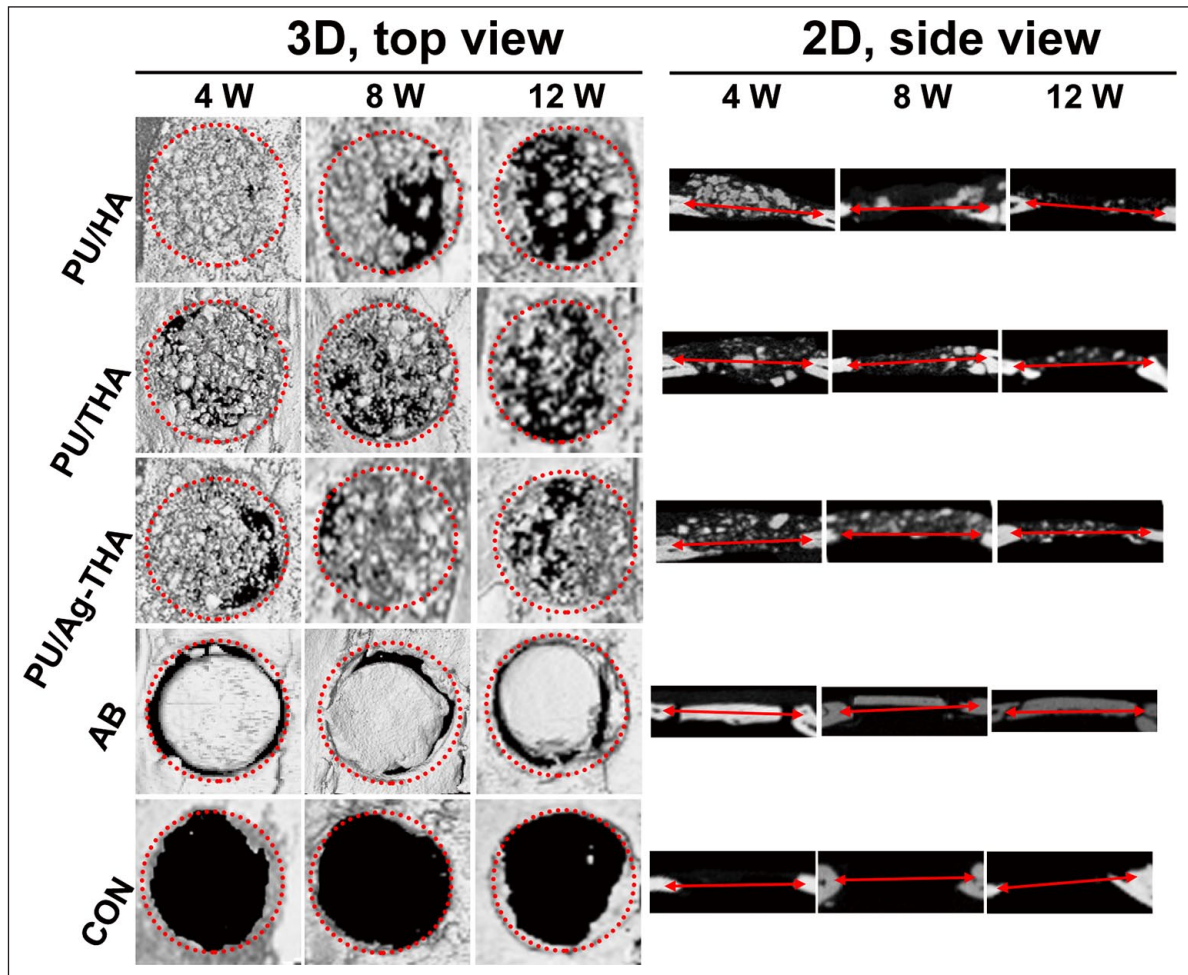
Figure 2. The representative reconstructed 3D (top view) and 2D (side view, midsagittal section) images of the treated calvarial defects for different groups collected at week 4, 8, 12 post surgery. The diameters of the red dotted cycles in the 3D images and lengths of the red colored arrows in the 2D images are all 5 mm.

Figure 1(b)) were also used for comparison, CON sample with the created defect being left untreated was also set.

After operation, the surgical incisions of all rats healed well, and there were no obvious postoperative complications such as redness and swelling, exudation and infection of wound; the activities of all rats were normal.

Micro-computed tomography (μ-CT) analysis

4, 8, and 12 weeks after operation, μ-CT analysis to the harvested tissue sections treated by PU/THA and PU/Ag-THA MPs was conducted, the bone mineral densities (BMDs) were calculated (Figure 1(d)) and the 3D and 2D images of the treated calvarial defects were also reconstructed (Figure 2). The highest level of peripheral bone formation was observed in the defects treated with AB compared to all other groups (Figure 1(d)), which is also evidenced by the radiopaque tissue bridging the implant and surrounding bone (Figure 2(a)). Although the BMD values at all the three time points of PU/THA and PU/

Ag-THA groups were lower than that of the AB group, they were all significantly higher than that of PU/HA and CON groups (Figure 1(d)). The reconstructed 3D and 2D images shown in Figure 2 also show the same trend (Figure 2). No significant differences were detected between the BMD values of PU/THA and PU/Ag-THA groups at all tested time points. These results indicate that the inclusion of tannin modified HA in bone composites promoted bone regeneration comparing to pure HA, agreeing the results that the inclusion of TA in CTBCs can enhance bone regeneration in our previous literature.[19] This may be attributed to the improved cell adhesion and biomineralization capability of THA comparing with that of pure HA.[19]

Histological analysis

To further study the bone regeneration effect of PU/THA and PU/Ag-THA MPs, H & E, Masson trichrome and Safranin O/fast green staining to the tissue sections harvested at week 4, 8, and 12 post surgery was also
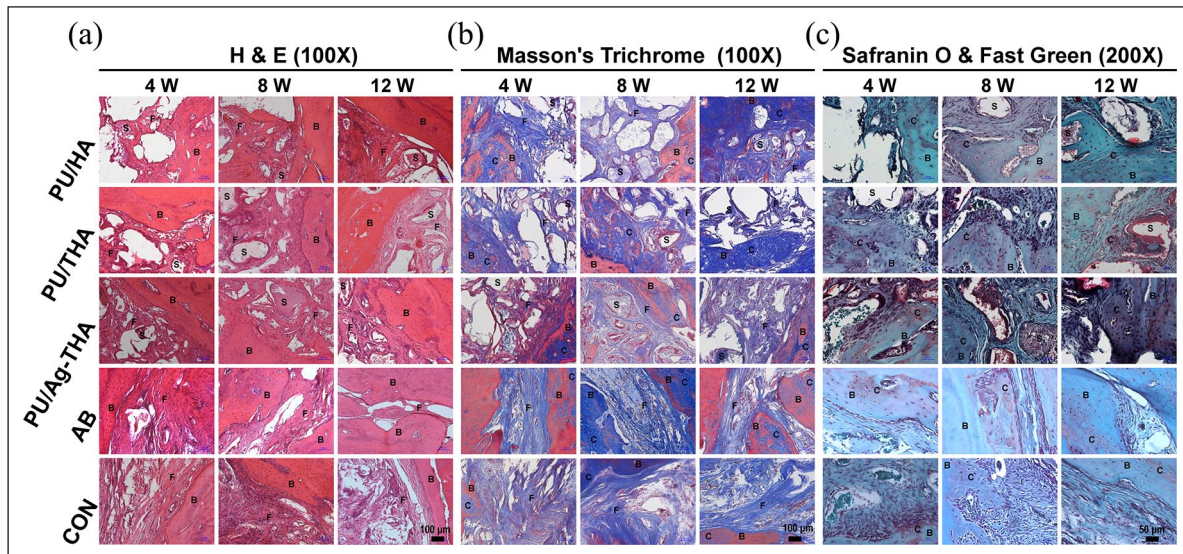
Figure 3. Representative histological staining images of the treated calvarial defect sections for PU/HA, PU/THA, PU/Ag-THA, AB and blank control (CON) groups 4, 8, and 12 weeks after operation. (a) H&E (hematoxylin and eosin) staining. (b) Masson's trichrome staining. (c) Safranin O & fast green staining.
B: bone; C: cartilage; F: fibrous tissue; S: scaffold.

conducted. The results are shown in Figure 3. In the AB group, the bone defect was filled with autogenous bone, and fibrous tissue connecting autogenous bone and the host bone can be observed (Figure 3(a)–(c)). While, in CON group, even at week 12, the bone defect was mostly filled with fibrous tissue, only a small amount of new bone can be found at the edge of the bone defect (Figure 3(a)–(c)). In the biomaterial groups, no obvious inflammatory cell infiltration was observed around the material (Figure 3(a)), proved the favorable biocompatibility of PU/THA and PU/Ag-THA. The implanted biomaterial was surrounded by fibrous tissue, neovascularization can be found surrounding the material. Along with the gradual degradation of biomaterials, more new bone tissue grew into the bone defect (Figure 3(a)–(c)). A large amount of cartilage tissue was observed in all samples, which is most evident by the Safranin O and fast green staining images where cartilage and bone tissue stains orange and green respectively (Figure 3(c)). This indicates that endochondral ossification might play an important role in calvarial regeneration process. Comparing with PU/HA and CON groups, the amounts of new bone tissue in the bone defects treated by PU/THA and PU/Ag-THA were higher than that in CON group consistent with the μ-CT results, further confirmed the favorable osteoconductivity of tannin modified HA, agreeing with the similar results obtained in the in vivo osteoconductivity study of tannin containing CTBCs in our previous literature.[19]

TRAP staining

To assess the activity of osteoclast during bone regeneration, TRAP staining was conducted. From Figure 4, it can
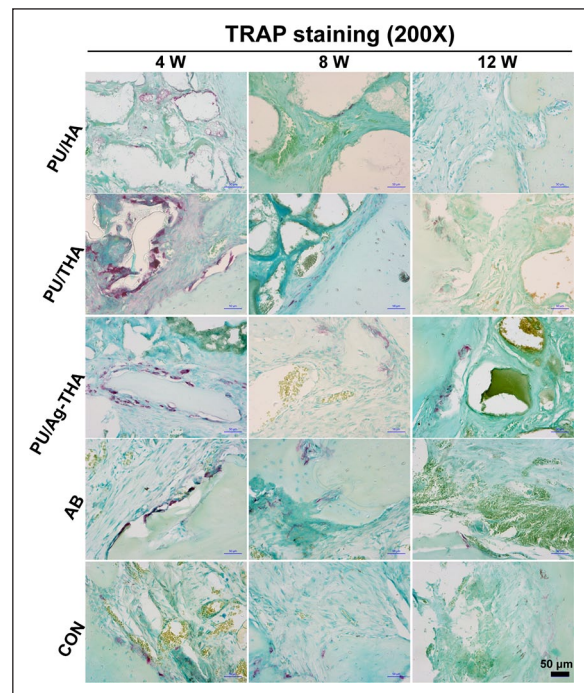

Figure 4. Representative tartrate resistant acid phosphatase (TRAP) staining images of the treated calvarial defect sections by different samples 4, 8, and 12 weeks after operation.

be seen that at week 4, the quantities of TRAP positive cells stain as purplish red in PU/HA, PU/THA, and PU/Ag-THA groups were much higher than that of AB and CON groups. TRAP positive cell nuclei aggregated together and displayed a shape of monster multi-nuclei osteoclast (Figure 4). At week 8 and 12, the quantity of
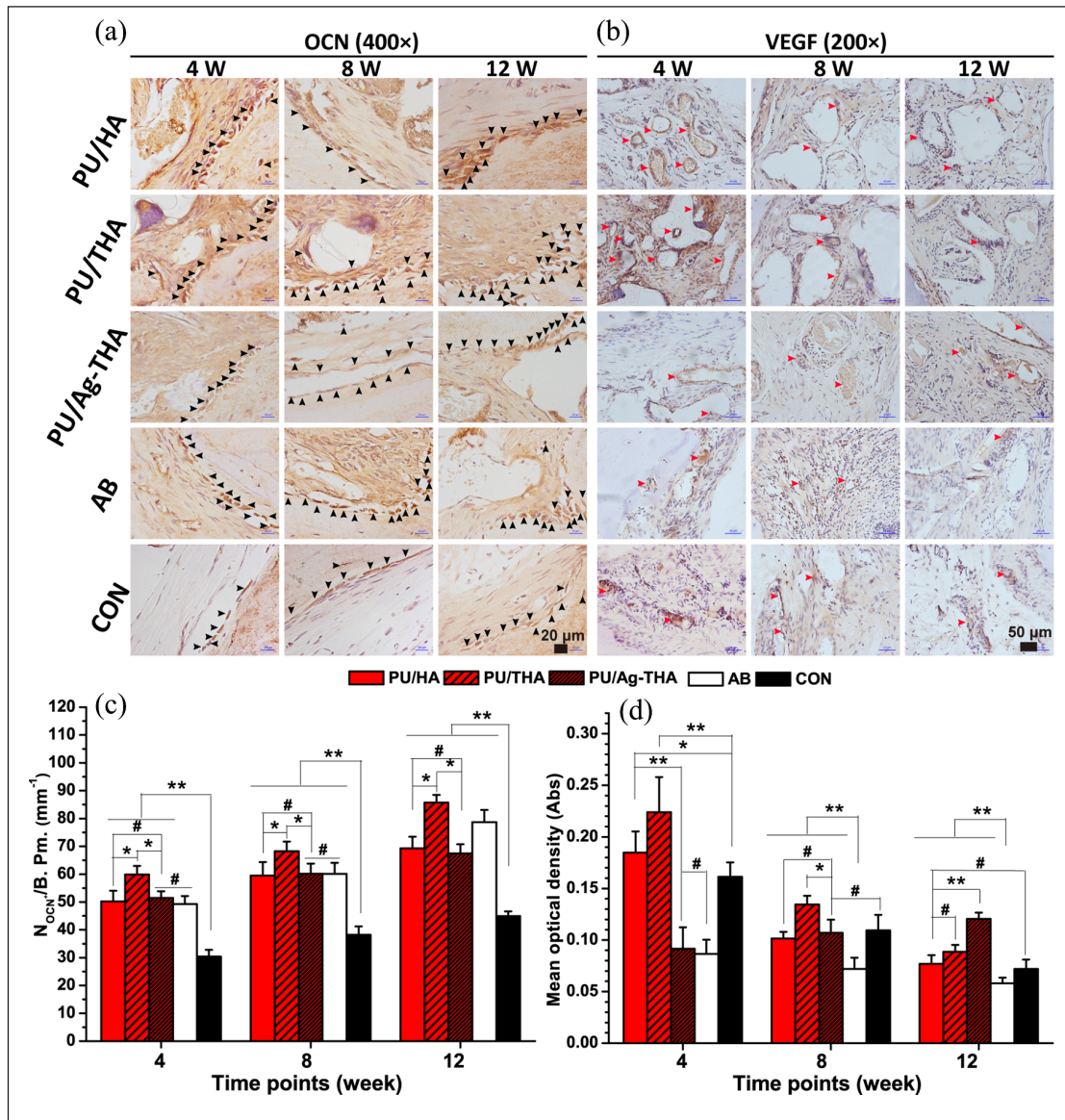
Figure 5. OCN (osteocalcin, a) and VEGF (vascular endothelial growth factor, b) immunohistochemical staining images of treated calvarial defects reflecting the osteogenesis and angiogenesis; The OCN and VEGF positive staining cells are pointed out using black and red color arrows respectively. The numbers of OCN (c) positive cells per mm length of bone perimeter (B. Pm.), and the mean optical densities of VEGF (d) positive cells calculated from OCN and VEGF staining images respectively.
$^{\#}p > 0.05$, $^{*}p < 0.05$, $^{**}p < 0.01$.

TRAP positive cells greatly reduced, demonstrating low osteoclast activity at later time points. These results indicate that high osteoclast activity is accompany with osteogenesis in the early stage, implying the critical importance of bone remodeling in bone regeneration, especially when foreign material was implanted. This can also be proved by the low activity of osteoclast throughout the whole bone regeneration process in AB sample.

Immunohistochemical staining

To further investigate the osteogenesis of PU/THA and PU/Ag-THA treated bone defects, immunohistochemical analysis of OCN were conducted (Figure 5(a)). OCN, as a non-collagen protein secreted by osteoblasts, is often used as a specific indicator of mature osteoblasts, thus OCN staining can reflect the osteoinductivity of the tested bone graft in some extent. From Figure 5(a)–(c), it can be seen that the numbers of OCN positive cells in PU/THA group were all significantly higher than that of PU/HA and CON groups. While, no significant difference was found between PU/HA and PU/Ag-THA groups, implying that the inclusion of Ag NPs impaired the osteoinductivity brought by TA (Figure 5(c)). The numbers of OCN positive cells in AB group at week 4 and 8 were even lower than that of biomaterial groups, this might due to the bone defect was filled transplanted autologous bone (Figure 5(c)).

On the other hand, it is proved that a large number of blood vessels and high expression of VEGF are produced in the mineralized area of cartilage during osteogenesis, indicating that vascular infiltration plays an important role in regulating the production of hypertrophic chondrocytes. Thus VEGF immunohistochemical staining reflecting the angiogenesis of the material was also conducted, the results are shown in Figure 5(b). VEGF positive cells were stained in brown color, and the optical densities of brown stained cells were also calculated. Obvious neovascularization can be found in the biomaterials treated bone defect samples (Figure 5(b)), which can also be evident by the significantly higher optical densities for PU/HA and PU/THA groups than AB and CON groups (Figure 5(d)). The optical densities of VEGF positive cells in PU/THA were significantly higher than that in PU/HA group, especially at week 4 and 8 (Figure 5(d)), indicating that the coating of TA on HA brought enhanced angiogenesis. While, the optical densities of VEGF positive cells in PU/Ag-THA group were significantly lower than that in PU/HA group (Figure 5(d)), implying that the further immobilization of Ag NPs on HA was harmful to the angiogenesis of THA. However, the angiogenesis ability of PU/Ag-THA recovered at week 12 (Figure 5(d)), at that time, most Ag NPs or silver ions might already be released into the microenvironment.

The OCN and VEGF staining results indicate that the inclusion of TA on HA enhanced the osteogenesis and angiogenesis, but the inclusion of Ag NPs should be controlled in some extent not to harm the angiogenesis of the material.

Conclusion

By compositing biocompatible and biodegradable polyurethane (PU) with tannic acid (TA) modified hydroxyapatite (HA) or silver nanoparticles (Ag NPs) & TA modified HA (Ag-THA). The grounded organic/inorganic PU/THA and PU/Ag-THA porous composite scaffold microparticles (MPs) were used for critical-sized calvarial regeneration on rats. The in vivo study confirmed the comparable biocompatibility of PU/THA and PU/Ag-THA composites with that of PU/HA, indicating that the inclusion of TA & Ag NPs on HA did not bring serious toxicity. PU/THA and PU/Ag-THA treated calvarial defects resulted in significantly higher bone mineral densities comparing with that of PU/HA and blank control (CON). The inclusion of TA on HA conferred the composites with enhanced osteogenesis and angiogenesis, evidenced by elevated osteocalcin (OCN) and vascular endothelial growth factor (VEGF) expression. High activity of osteoclast in early stage of material treated samples was evidenced from tartrate resistant acid phosphatase (TRAP) staining results, proved the important function of bone remodeling accompany with osteogenesis, especially when foreign material is implanted. Introduction of Ag NPs on HA depressed the angiogenesis of the composites in some extent, leading to even lower VEGF expression than that of CON group at week 4 and 8. This study proved that tannin modification of HA can enhance both osteogenesis and angiogenesis comparing to pure HA, while the introduction of antimicrobial Ag NPs on HA need to be controlled in some extent in order not to affect the angiogenesis of the composites. Furthermore, tannin modified HA still preserve a surface with multiple reacting functionalities, paving the way for additional surface biofuntionalization to further improve the biocompatibility and bioactivity.

ORCID iD

Zhihui Lu 🔟 https://orcid.org/0000-0001-5780-6863

References

1. Giannoudis PV, Dinopoulos H and Tsiridis E. Bone substitutes: an update. *Injury* 2005; 36(3): S20–S27.
2. Tang J, Guo J, Li Z, et al. A fast degradable citrate-based bone scaffold promotes spinal fusion. *J Mater Chem B* 2015; 3(27): 5569–5576.
3. Guo Y, Tran RT, Xie D, et al. Citrate-based biphasic scaffolds for the repair of large segmental bone defects. *J Biomed Mater Res A* 2015; 103(2): 772–781.
4. Parisi C, Salvatore L, Veschini L, et al. Biomimetic gradient scaffold of collagen–hydroxyapatite for osteochondral regeneration. *J. Tissue Eng* 2020; 11: 204173141989606.
5. Ma C, Tian X, Kim JP, et al. Citrate-based materials fuel human stem cells by metabonegenic regulation. *Proc Natl Acad Sci USA* 2018; 115(50): E11741–E11750.
6. Kohli N, Sawadkar P, Ho S, et al. Pre-screening the intrinsic angiogenic capacity of biomaterials in an optimised ex ovo chorioallantoic membrane model. *J Tissue Eng* 2020; 11: 204173142090162.
7. Sun D, Chen Y, Tran RT, et al. Citric acid-based osteoinductive scaffolds enhance calvarial regeneration. *Sci Rep* 2014; 4: 6912.
8. Wen G, Zhou R, Wang Y, et al. Management of post-traumatic long bone defects: a comparative study based on long-term results. *Injury* 2019; 50(11): 2070–2074.

9. Wubneh A, Tsekoura EK, Ayranci C, et al. Current state of fabrication technologies and materials for bone tissue engineering. *Acta Biomater* 2018; 80: 1–30.

10. Zhu T, Cui Y, Zhang M, et al. Engineered three-dimensional scaffolds for enhanced bone regeneration in osteonecrosis. *Bioact Mater* 2020; 5(3): 584–601.

11. Dong R, Bai Y, Dai J, et al. Engineered scaffolds based on mesenchymal stem cells/preosteoclasts extracellular matrix promote bone regeneration. *J Tissue Eng* 2020; 11: 204173142092691.

12. Cui L, Zhang J, Zou J, et al. Electroactive composite scaffold with locally expressed osteoinductive factor for synergistic bone repair upon electrical stimulation. *Biomaterials* 2020; 230: 119617.

13. Chahal AS, Schweikle M, Lian A-M, et al. Osteogenic potential of poly(ethylene glycol)-amorphous calcium phosphate composites on human mesenchymal stem cells. *J Tissue Eng* 2020; 11: 204173142092684.

14. Zhang Y, Liu X, Zeng L, et al. Polymer fiber scaffolds for bone and cartilage tissue engineering. *Adv Funct Mater* 2019; 29(36): 1903279.

15. Shao N, Guo J, Guan Y, et al. Development of organic/inorganic compatible and sustainably bioactive composites for effective bone regeneration. *Biomacromolecules* 2018; 19(9): 3637–3648.

16. Yang R, Chen F, Guo J, et al. Recent advances in polymeric biomaterials-based gene delivery for cartilage repair. *Bioact Mater* 2020; 5(4): 990–1003.

17. Guo J, Xie Z, Tran RT, et al. Click chemistry plays a dual role in biodegradable polymer design. *Adv Mater* 2014; 26(12): 1906–1911.

18. Wu D, Zhao P, Wu L, et al. Aptamer-functionalized gold nanostars for on-demand delivery of anticancer therapeutics. *ACS Appl Bio Mater* 2020; 3(7): 4590–4599.

19. Guo J, Tian X, Xie D, et al. Citrate-based tannin-bridged bone composites for lumbar fusion. *Adv Funct Mater* 2020; 30(27): 2002438.

20. Hofmann A, Ritz U, Verrier S, et al. The effect of human osteoblasts on proliferation and neo-vessel formation of human umbilical vein endothelial cells in a long-term 3D co-culture on polyurethane scaffolds. *Biomaterials* 2008; 29(31): 4217–4226.

21. Guelcher SA. Biodegradable polyurethanes: synthesis and applications in regenerative medicine. *Tissue Eng Part B Rev* 2008; 14(1): 3–17.

22. Marzec M, Kucinska-Lipka J, Kalaszczynska I, et al. Development of polyurethanes for bone repair. *Mater Sci Eng C* 2015; 7: 24641–24648.

23. Qiu X, Chen L, Hu J, et al. Surface-modified hydroxyapatite linked by L-lactic acid oligomer in the absence of catalyst. *J Polym Sci A Polym Chem* 2005; 43(21): 5177–5185.

24. Wang Z, Chen L, Wang Y, et al. Improved cell adhesion and osteogenesis of op-HA/PLGA composite by poly(dopamine)-assisted immobilization of collagen mimetic peptide and osteogenic growth peptide. *ACS Appl Mater Interfaces* 2016; 8(40): 26559–26569.

25. Wei J, Liu A, Chen L, et al. The surface modification of hydroxyapatite nanoparticles by the ring opening polymerization of γ-Benzyl-L-glutamate N-carboxyanhydride. *Macromol Biosci* 2009; 9(7): 631–638.

26. Wei J, He P, Liu A, et al. Surface modification of hydroxyapatite nanoparticles with thermal-responsive PNIPAM by ATRP. *Macromol Biosci* 2009; 9(12): 1237–1246.

27. Sileika TS, Barrett DG, Zhang R, et al. Colorless multifunctional coatings inspired by polyphenols found in tea, chocolate, and wine. *Angew Chem Int Ed Engl* 2013; 52(41): 10766–10770.

28. Niu Y, Chen KC, He T, et al. Scaffolds from block polyurethanes based on poly(ε-caprolactone) (PCL) and poly(ethylene glycol) (PEG) for peripheral nerve regeneration. *Biomaterials* 2014; 35(14): 4266–4277.

29. Niu Y, Li L, Chen KC, et al. Scaffolds from alternating block polyurethanes of poly(ε-caprolactone) and poly(ethylene glycol) with stimulation and guidance of nerve growth and better nerve repair than autograft. *J Biomed Mater Res A* 2015; 103(7): 2355–2364.

30. Li L, Liu X, Niu Y, et al. Synthesis and wound healing of alternating block polyurethanes based on poly(lactic acid) (PLA) and poly(ethylene glycol) (PEG). *J Biomed Mater Res B* 2017; 105(5): 1200–1209.

31. Hollinger JO and Kleinschmidt JC. The critical size defect as an experimental model to test bone repair materials. *J Craniofac Surg* 1990; 1(1): 60–68.